

Micro-sized cold atmospheric plasma source for brain and breast cancer treatment

Zhitong Chen¹, Li Lin¹, Qinmin Zheng², Jonathan H. Sherman³, Jerome Canady⁴, Barry Trink⁵,
Michael Keidar^{1*}

¹Department of Mechanical and Aerospace Engineering, The George Washington University,
Washington, DC 20052, USA

²Department of Civil and Environmental Engineering, The George Washington University,
Washington, DC 20052, USA

³Department of Neurosurgery, The George Washington University, Washington, DC 20052,
USA

⁴Jerome Canady Research Institute for Advanced Biological and Technological Sciences, US
Medical innovation LLC, Takoma Park, MD 20912, USA

⁵Department of Otolaryngology, School of Medicine, Johns Hopkins University, Baltimore,
Maryland 21205, USA

* Corresponding Author:
[E-mail address: zhitongchen@gwu.edu](mailto:zhitongchen@gwu.edu), keidar@gwu.edu

Abstract

Micro-sized cold atmospheric plasma (μ CAP) has been developed to expand the applications of CAP in cancer therapy. In this paper, μ CAP devices with different nozzle lengths were applied to investigate effects on both brain (glioblastoma U87) and breast (MDA-MB-231) cancer cells. Various diagnostic techniques were employed to evaluate the parameters of μ CAP devices with different lengths such as potential distribution, electron density, and optical emission spectroscopy. The generation of short- and long-lived species (such as hydroxyl radical (\bullet OH), superoxide (O_2^-), hydrogen peroxide (H_2O_2), nitrite (NO_2^-), et al) were studied. These data revealed that μ CAP treatment with a 20 mm length tube has a stronger effect than that of the 60 mm tube due to the synergetic effects of reactive species and free radicals. Reactive species generated by μ CAP enhanced tumor cell death in a dose-dependent fashion and was not specific with regards to tumor cell type.

Key words: Micro-sized, Cold atmospheric plasma, Reactive species, Breast cancer, Glioblastoma cancer, cancer therapy

Introduction

Cold atmospheric plasma (CAP) has been proposed as a novel therapeutic method for anticancer treatment, which can be applied to living tissues and cells^{1,2}. CAP is a partially ionized gas that contains charge particles, reactive oxygen and nitrogen species (ROS and RNS), excited atoms, free radicals, UV photons, electric field, etc^{3,4}. ROS and RNS, combined or independently, are well known to initiate different signaling pathways in cells and to promote oxidative stress^{5,6}. Plasma-induced biological effects include damage to lipids, proteins, DNA, and induce apoptosis through plasma-generated ROS and RNS⁷⁻¹⁰. Moreover, many studies have reported both *in vivo* and *in vitro* that plasma is a possible adjunct treatment in oncology as well as killing achieved for various types of cancers such as glioblastoma, breast cancer, bladder carcinoma, cervical carcinoma, skin carcinoma, pancreatic carcinoma, lung carcinoma, colon carcinoma, gastric carcinoma, melanoma and hepatocellular carcinoma¹¹⁻²⁷.

In plasma medicine, jet plasma, corona discharge, and dielectric barrier discharge (DBD) have been used²⁸. These types of plasma can be directly applied to skin cancers, while they are not applicable for more systemic cancer treatment. Some studies investigated the plasma device in the micro-sized to conduct the plasma species to the living animals²⁹. However, their device just applied to xenografts tumors not systemic cancer treatment. Moreover, delivery of the plasma species is crucial to suppress tumor growth and assess efficiency of micro-sized plasma device. Hence, this study aims to design micro-sized cold atmospheric plasma devices with different lengths of nozzle in order to enhance delivery of reactive species and evaluate the efficiency of these devices on cancer therapy. Fig. 1 shows the potential applications of μ CAP for brain and breast tumors in the future.

Brain Cancer

Breast Cancer

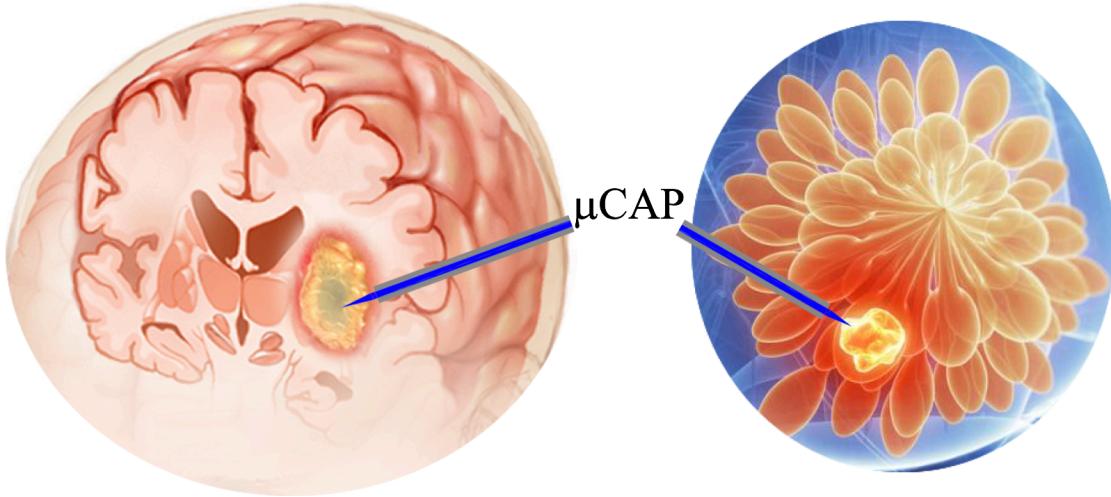


Figure 1. Potential applications of μ CAP for brain and breast tumors

Materials and Methods

Fig. 2 depicts the schematic of the experiment setup including high voltage power (Fig. 2a) and μ CAP devices (Fig. 2b). The high voltage power includes DC input, Trigger signal + MOSFET (switch), and the secondary output. In this work, the DC input was set at 5 V, square wave signal was obtained from the control unit (upper left in Fig. 2a), and a high voltage wave was obtained from the square wave signal through the transformer (upper right in Fig. 2a). The μ CAP devices consist of a two-electrode (copper) assembly with a central powered electrode (1 mm in diameter) and a grounded outer electrode wrapped around the outside of a quartz tube (10 mm) as shown in Fig. 2b. The electrodes were connected to the secondary output of the high voltage transformer. The peak-peak voltage was approximately 8 kV and the frequency of the discharge was around 16 kHz (upper right in Fig. 2a). The secondary output of high voltage transformer was connected to the first input. At the end of a quartz tube, a $275 \pm 5 \mu\text{m}$ inner diameter capillary tube (stainless steel) with 20 or 60 mm length was attached and insulated by epoxy. The feed gas for this study was industrial purity helium, which was injected into the quartz tube with a 0.2 L/min gas flow rate. Longer tube (60 mm) is needed to access deeper tumors in brain and breast. In this study, we are accessing effect of length to understand limitation of depth.

In this study, we are assessing the effect of tube length to understand limitation of depth. For instance, it is believed that a longer tube (60 mm) is needed to access deeper tumors in brain and breast. UV-visible-NIR, a range of wavelength 200-850 nm, was investigated on plasma to detect various RNS and ROS (nitrogen [N_2], nitric oxide [$-\text{NO}$], nitrogen cation [N^{+2}], atomic oxygen [O], and hydroxyl radicals [$-\text{OH}$]). The optical probe was placed at distance of 1.0 cm in front of the plasma jet nozzle. Data were then collected with an integration time of 100 ms.

A fluorimetric hydrogen peroxide assay Kit (Sigma-Aldrich) was used for measuring the amount of H₂O₂, according to the manufacturer's protocol. Briefly, 50 μ l of standard curve, control, and experimental samples were added to 96-well flat-bottom black plates, and then 50 μ l of Master Mix was added to each of well. The plates were incubated for 20 min at room temperature protected from light and fluorescence was measured by a Synergy H1 Hybrid Multi-Mode Microplate Reader at Ex/Em: 540/590 nm.

RNS level were determined by using a Griess Reagent System (Promega Corporation) according to the instructions provided by the manufacturer. Briefly, 50 μ l of samples and 50 μ l of the provided Sulfanilamide Solution were added to 96-well flat-bottom plates and incubated for 5-10 minutes at room temperature. Subsequently, 50 μ l of the NED solution was added to each well and incubated at room temperature for 5-10 minutes. The absorbance was measured at 540 nm by Synergy H1 Hybrid Multi-Mode Microplate Reader.

XTT sodium salt ((2,3-bis(2-methoxy-4-nitro-5-sulphophenyl)-5-[(phenylamino)carbonyl]-inner salt-2H-tetrazolium, monosodium salt)) solution, purchased from Cayman chemical, was prepared by dissolving XTT power in DMEM. XTT sodium salt solution (100 μ l per well, 500 μ M) in a 96-well flat-bottom plate by μ CAP for 5, 10, 30, 60, and 120 seconds. The gap between the outlet of μ CAP and the surface of the samples was set at approximately 3 mm. As a control, untreated XTT sodium salt solution in triplicate were transferred to a 96-well flat-bottom plate. As a control, DMEM (100 μ l per well) was treated with μ CAP for 5, 10, 30, 60, and 120 seconds. The color change of XTT solution was used to indicate the presence of superoxide (O₂⁻). A color change of XTT solution was measured by Hach DR 6000 uv vis spectrophotometer at 470 nm.

A MB solution was prepared by dissolving MB power in DMEM. MB solutions (100 μ l per well, 0.01g/L) in a 96-well flat-bottom plate were treated by μ CAP for 5, 10, 30, 60, and 120 seconds.

The gap between the outlet of μ CAP and the surface of the samples was approximately 3 mm. As a control, untreated MB solutions in triplicate were transferred to a 96-well flat-bottom plate. The color change of methylene blue shows the presence of OH radicals via immediate and distinct bleaching of methylene blue dye (qualitatively analysis). The color change of the MB solution was measured as the absorbance at 664 nm by a Synergy H1 Hybrid Multi-Mode Microplate Reader.

Human glioblastoma cancer cells (U87MG, Perkin Elmer) were cultured in Dulbecco's Modified Eagle Medium (DMEM, Life Technologies) supplemented with 10% (v/v) fetal bovine serum (Atlantic Biologicals) and 1% (v/v) penicillin and streptomycin (Life Technologies). Cultures were maintained at 37°C in a humidified incubator containing 5% (v/v) CO₂. The human breast cancer cell line (MDA-MB-231) was cultured in Dulbecco's Modified Eagle Medium (DMEM, Life Technologies) supplemented with 10% (v/v) foetal bovine serum (Atlantic Biologicals) and 1% (v/v) penicillin and streptomycin (Life Technologies). Cultures were maintained at 37 °C in a humidified incubator containing 5% (v/v) CO₂.

U87 and MDA-MB-231 cells were plated in 96-well flat-bottom microplates at a density of 3000 cells per well in 100 μ L of complete culture medium. Cells were incubated for 24 hours to ensure proper cell adherence and stability. On day 2, the cells were treated by He μ CAP for 0, 5, 10, 30, 60, and 120 seconds. Cells were further incubated at 37°C for 24 and 48 hours. The cell viability of the glioblastoma and breast cancer cells were measured for each incubation time point with an MTT assay. 100 μ L of MTT solution (3-(4, 5-dimethylthiazol-2-yl)-2,5-diphenyltetrazolium bromide) (Sigma-Aldrich) was added to each well followed by a 3-hour incubation. The MTT solution was discarded and 100 μ L per well of MTT solvent (0.4% (v/v) HCl in anhydrous isopropanol) was added to the wells. The absorbance of the purple solution was recorded at 570 nm with a Synergy H1 Hybrid Multi-Mode Microplate Reader.

Results and Discussion

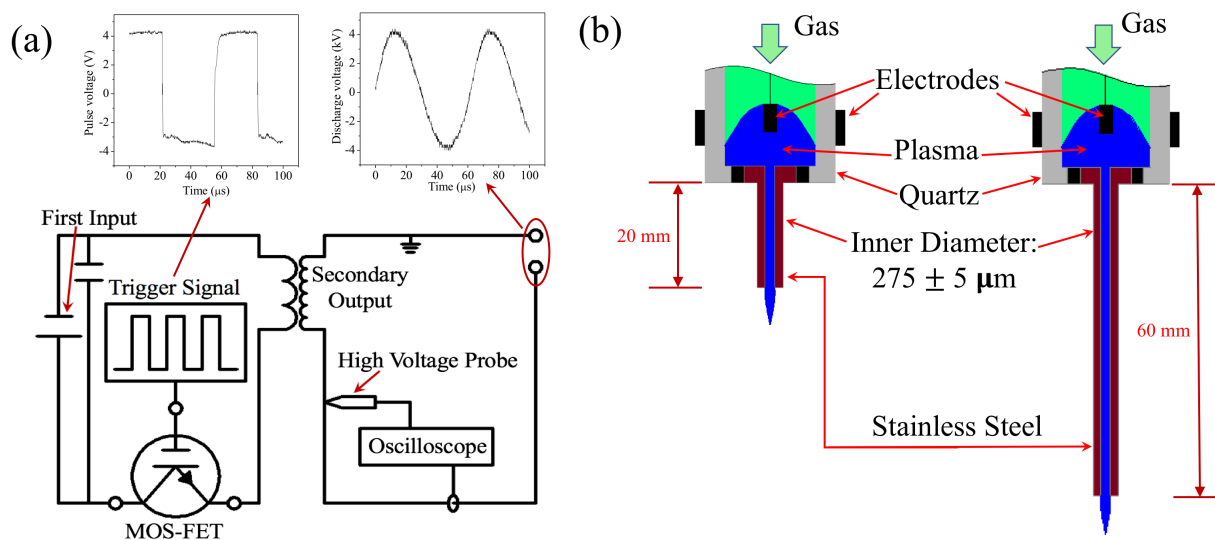


Figure 2. Schematic representation of the experiment setup including high voltage power part (a) and the micro-sized cold atmospheric plasma with 20 mm and 60 mm length of stainless steel tubes (b).

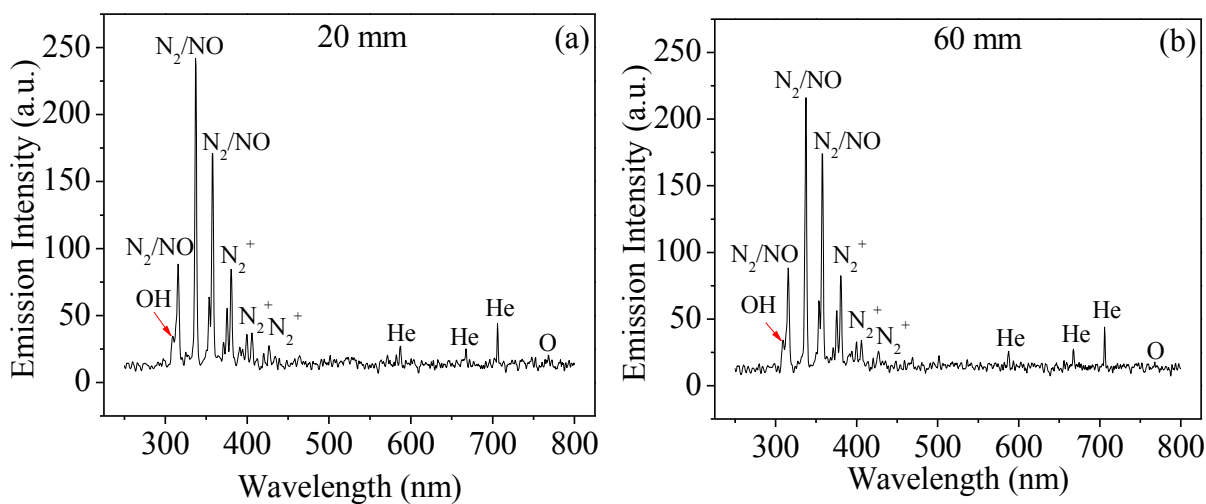


Figure 3. Optical emission spectrum detected from the He μ CAP with 20mm (a) and 60 mm (b) length's tube using UV-visible-NIR, in the 250–850 nm wavelength range.

The reactive species generated by the μ CAP device with different micro-sized tube length are detected by optical emission spectroscopy, as shown in Fig. 3. The identification of the emission line and bands was performed mainly according to reference³⁰. For 20 mm and 60 mm length devices, an N₂ second-positive system (315 nm, 337 nm 357 nm, and 380 nm) representing the photon emission intensity drops from the state C³Π_u to β³Π_g with different upper and lower

vibration quantum numbers. There are very weak emission lines in the special range of 250-300 nm, which are detected as NO lines. The helium bands were assigned between 500 and 750 nm as shown in Fig. 3a and 3b. We also observed a high-intensity OH/O₃ peak at 309 nm for both 20 mm and 60 mm length devices. Atomic oxygen (O, including the ground state and all the excited states of atomic oxygen) was observed at 777 nm in both devices, which was believed to have a significant effect on cells and therefore a broad biomedical application. Micro-sized plasma is a complicated environment that combines the comprehensive effect of different ions and reactive species. The 60 mm μ CAP has a bit less electron and species than 20 mm μ CAP due to long distance delivery.

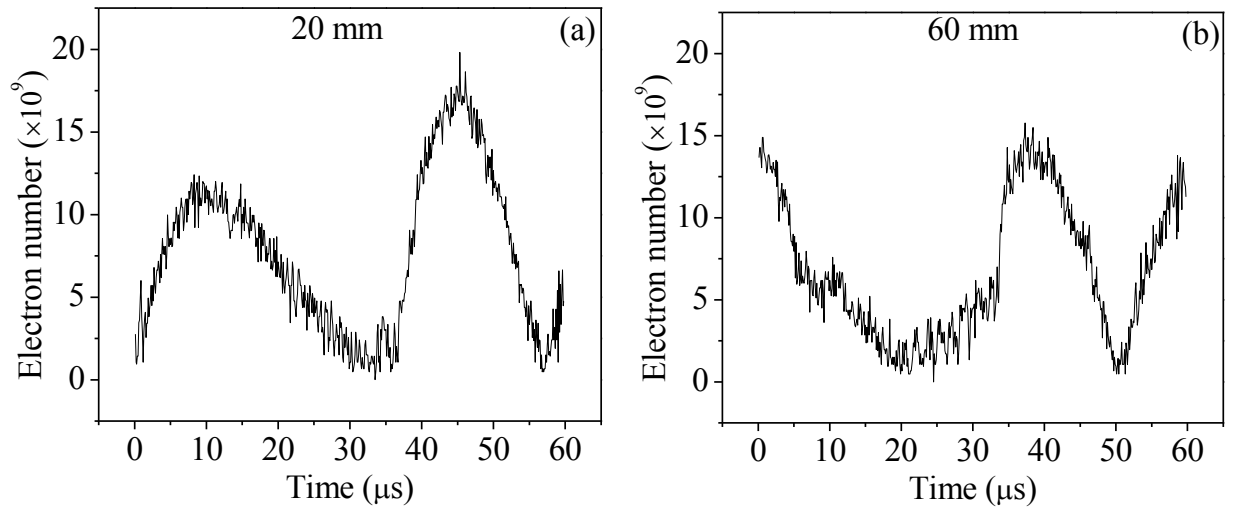


Figure 4 The electron number of 20 mm (a) and 60 mm (b) length μ CAP

The experimental Rayleigh microwave scattering (RMS) system was described previously¹⁹. The detection of the scattered signal was accomplished using a homodyne scheme by means of an I/Q mixer, providing in-phase (I) and quadrature (Q) outputs. For the entire range of scattered signals, the amplifiers and mixer were operated in linear mode. The total amplitude of the scattered microwave signal was determined by: $U = \sqrt{I^2 + Q^2}$. We can calculate the total electron number in the plasma as $N_e = U(w^2 + v_m^2)/(2.82 \times 10^{-4} A v_m)$, where w is the angular frequency, v_m is

the frequency of the electron-neutral collisions, and A is the proportionality coefficient³¹. The total electron number in the jet from μ CAP with 20 mm and 60 mm is presented in Fig. 4a and 4b, and the total electron number for one discharge period is 4.60×10^{12} and 4.04×10^{12} , respectively. A very small decrease of electron number has been detected in 60 mm μ CAP comparing with 20 mm μ CAP.

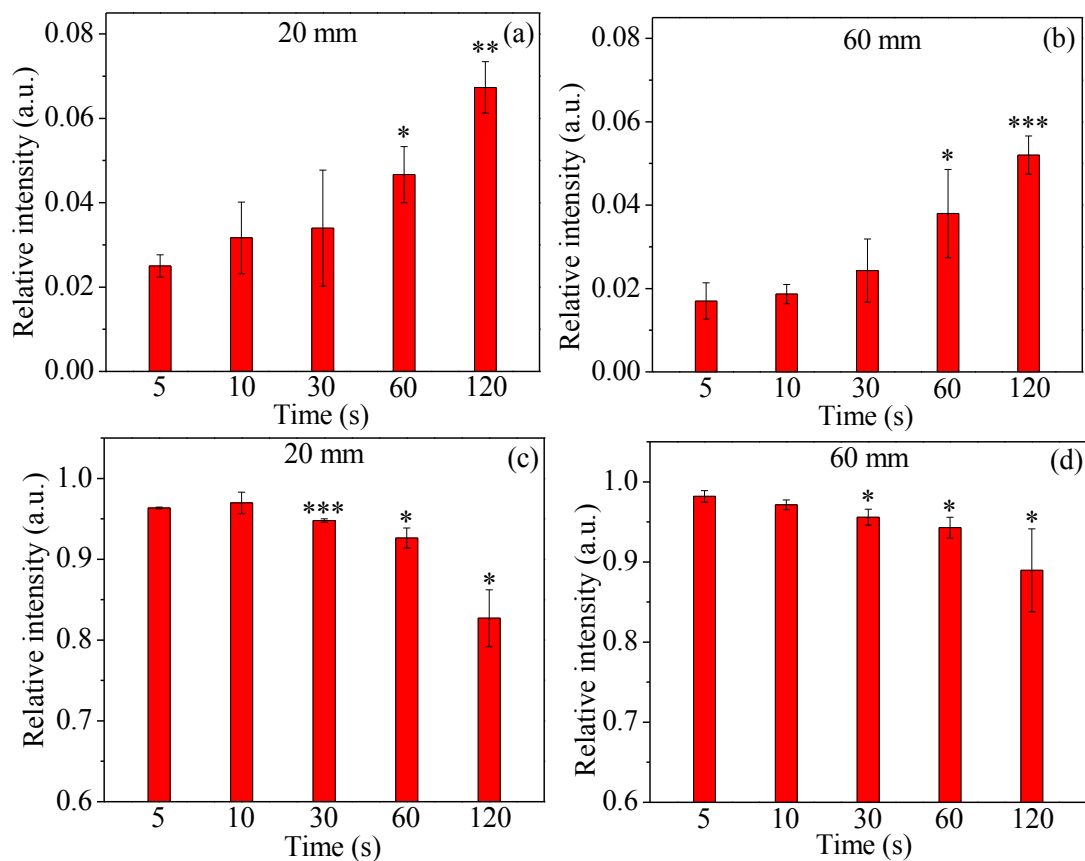


Figure 5. Relative O_2^- and $\bullet OH$ concentration of 20 mm and 60 mm μ CAP-treated DMEM. For relative O_2^- concentration: (a) 20 mm and (b) 60 mm. For relative $\bullet OH$ concentration: (c) 20 mm and (d) 60 mm. Student t-test was performed, and the statistical significance compared to μ CAP 5 s treatment is indicated as * $p < 0.05$, ** $p < 0.01$, *** $p < 0.001$. ($n = 3$).

XTT solution was used to determine the relative concentration of superoxide (O_2^-). Superoxide radical reduced soluble formazans of the tetrazolium dye XTT^{32,33}. Fig. 5a and 5b shows the relative superoxide concentration of 20 mm and 60mm μ CAP treatment of DMEM. Relative intensity increases with treatment, which corresponds to the relative concentration of superoxide

increasing with treatment. Comparing the 20 mm with 60 mm lengths, the 20 mm μ CAP device produced a higher relative concentration of superoxide than the 60 mm device. Methylene blue (MB) was used to assess the relative concentration of hydroxyl radicals (\bullet OH). It is known that MB reacts with \bullet OH aqueous solutions, leading to a visible color change³⁴. Fig. 5c and 5d shows that the relative MB concentration decreases with the treatment time of μ CAP, suggesting that more \bullet OH species are generated in DMEM (20 mm > 60 mm). Overall, these findings demonstrate that there is an increase in the relative concentration of O_2^- and \bullet OH as a function of μ CAP treatment time.

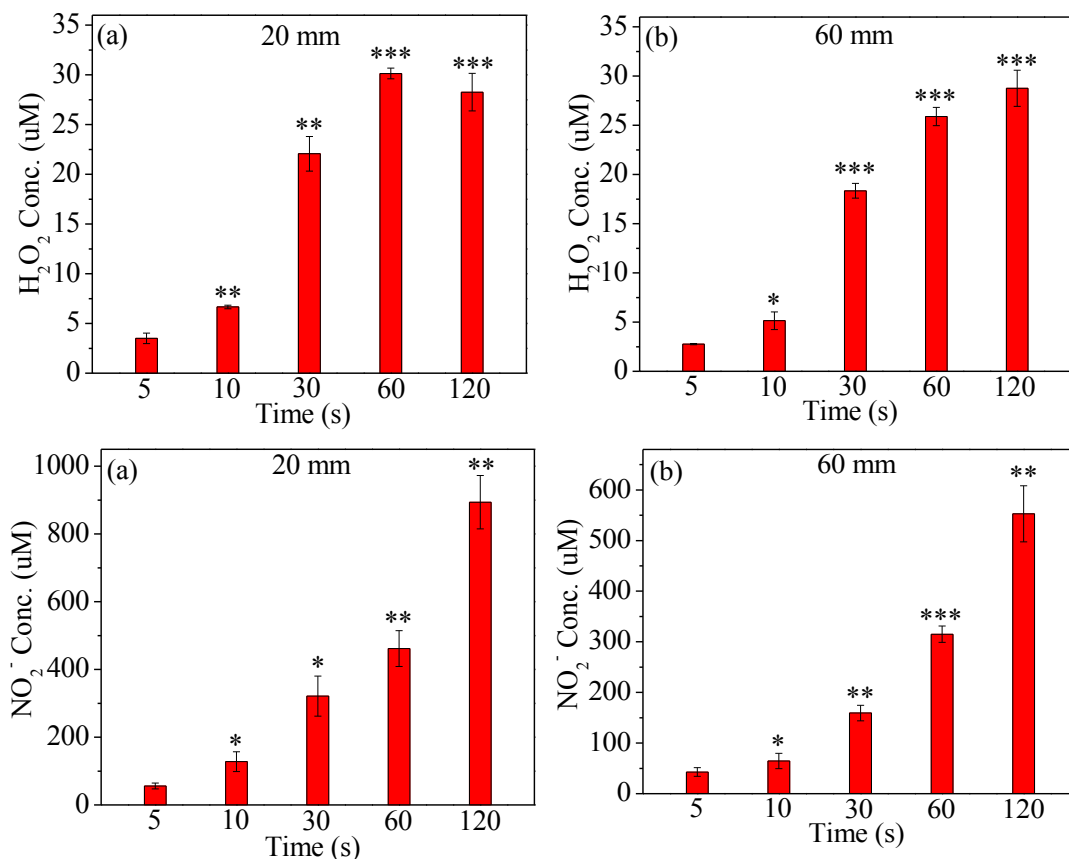


Figure 6. H_2O_2 and NO_2^- concentration of 20 mm and 60 mm μ CAP-treated DMEM. For H_2O_2 concentration: (a) 20 mm and (b) 60 mm. For NO_2^- concentration: (c) 20 mm and (d) 60 mm. Student t-test was performed, and the statistical significance compared to μ CAP 5 s treatment is indicated as * $p < 0.05$, ** $p < 0.01$, *** $p < 0.001$. (n = 3).

DMEM treated by the 20 mm and 60 mm μ CAP induced changes in the concentration of H_2O_2 and NO_2^- as a function of the treatment time. These results are shown in Fig. 6 with concentrations produced by the 20 mm and 60 mm He μ CAP devices. In Fig. 6a, the H_2O_2 concentrations produced by 20 mm He μ CAP device increase with treatment time up to 60 seconds, but between 60 seconds and 120 seconds the concentration decreased. For the H_2O_2 concentration produced by 60 mm He μ CAP increased with treatment time (In Fig. 6b). It means that the H_2O_2 concentration earlier reaches saturation in 20 mm length earlier than with the 60 mm length μ CAP device. In Fig. 5, we know that He μ CAP produces $\bullet\text{OH}$ and O_2^- in DMEM, which are the two most important species in plasma-activated media. In particular, $\bullet\text{OH}$ reacting with $\bullet\text{OH}$ and O_2^- reacting with 2H^+ lead to H_2O_2 formation³⁵. Both NO_2^- concentrations of 20 mm and 60 mm increase with treatment time (in Fig. 6c and Fig. 6d), and NO_2^- concentrations of 20 mm is much higher than 60mm. Comparing NO_2^- concentration with the H_2O_2 concentration under same condition, NO_2^- concentration is much higher than H_2O_2 concentration. A possible hypothesis for this result is that DMEM comprises over 30 components such as inorganic salts, amino acids and vitamins, and plasma might react with amino acids to form NO_2^- .

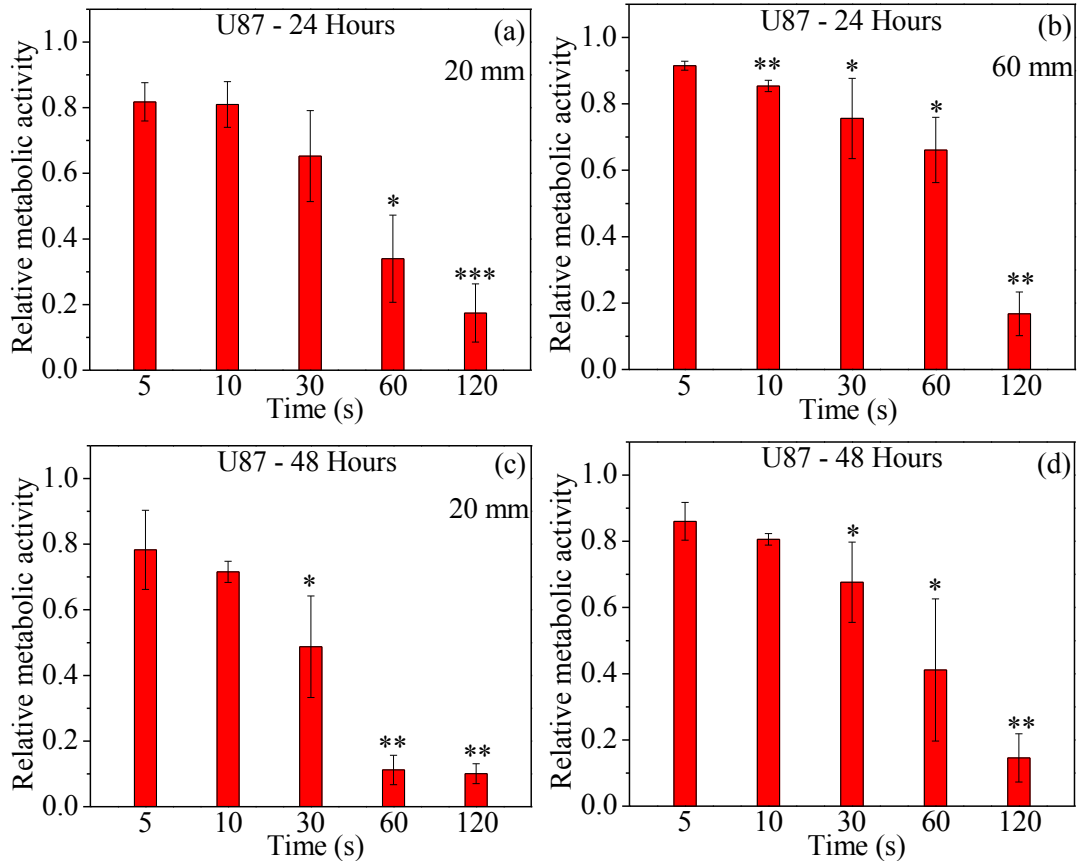


Figure 7. Cell viability of U87 after 24 and 48 hours' incubation with μ CAP treatment with 20 mm and 60 mm length during 5, 10, 30, 60, and 120 seconds' treatment. Cell viability of U87 treated by 20 mm He μ CAP at (a) 24-h incubation and (c) 48-h incubation. Cell viability of U87 treated by 60 mm He μ CAP at (b) 24-h incubation and (d) 48-h incubation. The ratios of surviving cells for each cell line were normalized relative to controls (DMEM). Student t-test was performed, and the statistical significance compared to cells present in DMEM is indicated as * $p < 0.05$, ** $p < 0.01$, *** $p < 0.005$. (n=3)

Fig. 7 shows the cell viability of the brain (glioblastoma U87) cancer cells after 24 and 48 hours' incubation with μ CAP during 5, 10, 30, 60, and 120 seconds' treatment with the 20 mm and 60 mm length μ CAP device, respectively. For the 20 mm length μ CAP treatment, the cell viability of brain cancer cells was lower than that of the 60 mm length at each treatment duration (from 5 to 60 seconds), and dropped with increasing treatment time. For both 20 mm and 60 mm, 120 seconds' treatment has similar effect on cell viability of U87 cancer cells. For 48 hours' incubation under 20 mm μ CAP treatment, 60 and 120 seconds' duration has similar effect on cell viability. Thus, overall conclusion is that 60mm tube can still produce reactive species while allowing access to

deeper tumors.

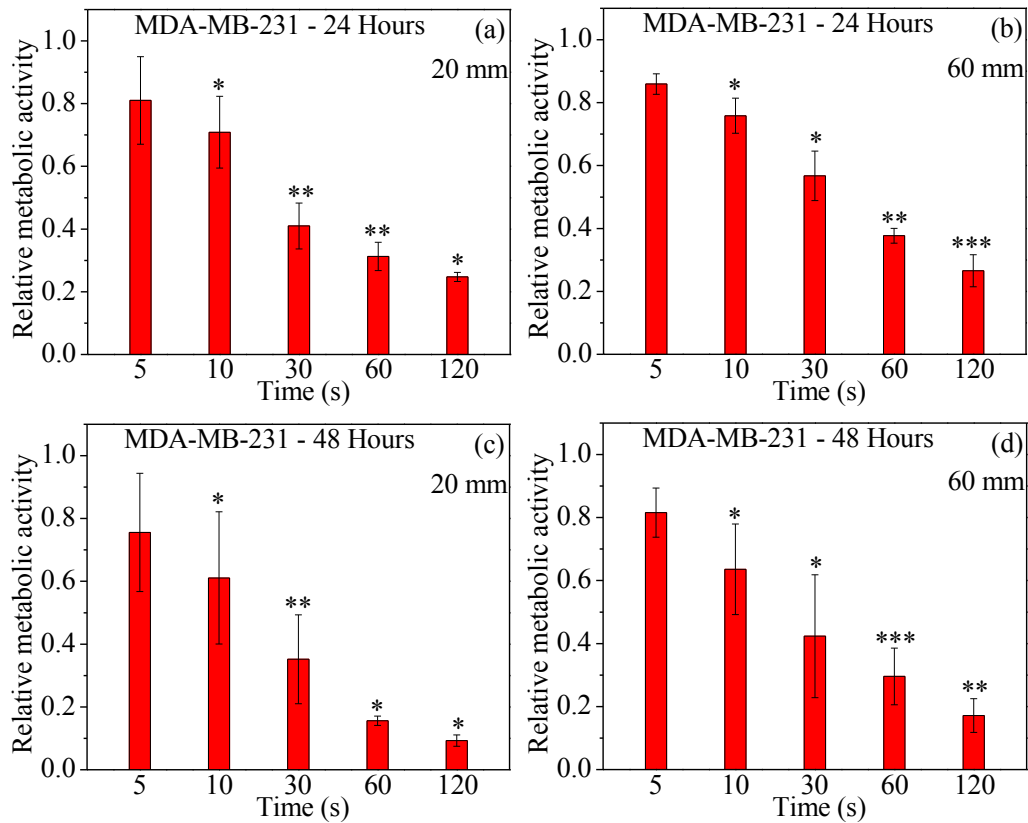


Figure 8. Cell viability of MDA-MB-231 after 24 and 48 hours' incubation with μ CAP treatment with 20 mm and 60 mm length during 5, 10, 30, 60, and 120 seconds' treatment. Cell viability of MDA-MB-231 treated by 20 mm He μ CAP at (a) 24-h incubation and (c) 48-h incubation. Cell viability of MDA-MB-231 treated by 60 mm He μ CAP at (b) 24-h incubation and (d) 48-h incubation. The ratios of surviving cells for each cell line were calculated relative to controls (DMEM). Student t-test was performed, and the statistical significance compared to cells present in DMEM is indicated as * $p < 0.05$, ** $p < 0.01$, *** $p < 0.005$. ($n=3$)

Fig. 8 shows the cell viability of the breast (MDA-MB-231) cancer cells after 24 and 48 hours' incubation with μ CAP treatment with the 20 mm and 60 mm length μ CAP devices during 5, 10, 30, 60, and 120 seconds' duration. For both 20 mm and 60 mm μ CAP treatment, the cell viability after 24 and 48 hours' incubation dropped with increasing treatment time. For 20 mm μ CAP treatment, the cell viability of breast cancer cells was lower than that of the 60 mm length at each treatment duration.

The direct plasma jet irradiation is limited to the skin and it can also be invoked as a supplement therapy during surgery as it only causes cell death in the upper three to five cell layers. However,

the current cannulas from which the plasma emanates are too large for intracranial applications. Thus, we developed a micro-sized plasma devices with 20 mm and 60 mm length stainless steel tubes, which both can achieve effective killing of brain and breast cancer cells. This preliminary study offers significant potential for new treatment applications. Numerous studies reported plasma-induced apoptosis in cancer cells due to plasma-generated various reactive species^{1,36,37}. Plasma generates various kinds of ROS and RNS, including hydrogen peroxide (H₂O₂), ozone (O₃), hydroxyl radical (•OH), atomic oxygen (O), superoxide (O₂⁻), nitric oxide (NO) and peroxy nitrite anion (ONOO⁻), singlet delta oxygen (O₂(¹Δg)), nitrite (NO₂⁻)^{37,38} and are displayed in Fig. 3. In this paper, we have specifically measured relative concentrations of O₂⁻ and •OH (short-lived species, Fig. 5) and the concentration of H₂O₂ and NO₂⁻ (long-lived species, Fig. 6). The relative concentration of O₂⁻ treated by μCAP with 20 mm and 60 mm increases with treatment time (Fig. 5a and 5b). O₂⁻ can activate mitochondrial-mediated apoptosis by changing mitochondrial membrane potential and simultaneously up-regulates pro-apoptotic genes and down-regulates anti-apoptotic genes for activation of caspases resulting in cell death³⁹. Fig. 5c and 5d shows the relative concentration of •OH in DMEM treated by μCAP with 20 mm and 60 mm also increases with treatment time. •OH derived amino acid peroxides can contribute to cell injury because •OH itself and protein (amino acid) peroxides are able to react with DNA, thereby inducing various forms of damage⁴⁰. Compared with cell viability of both cancer lines, the trend of cell death can be partly attributed to the increase of O₂⁻ and •OH concentration with treatment time. On the other hand, the 20 mm μCAP device shows higher relative concentrations of O₂⁻ and •OH, such that the 20 mm μCAP device is more effective in killing both cancer cell lines than the 60 mm μCAP device. Fig. 6 shows H₂O₂ and NO₂⁻ concentration of the 20 mm and 60 mm μCAP-treated DMEM. H₂O₂ can induce cell death by apoptosis and necrosis, while NO₂⁻ are known to induce cell death via DNA

damage^{36,41}. Thus, the synergism of H_2O_2 and NO_2^- might be an important factor in cancer cells killing efficiency.

Several methods are now being used for the cancer treatment such as chemotherapy, surgery, and radiotherapy⁴²⁻⁴⁴. The conventional methods have some disadvantages such as low rapidity, high cost, and adverse effects. However, plasma treatment may overcome these disadvantages of the traditional treatments. Currently, plasma can be directly applied to skin cancers, while it is not applicable for more systemic cancer treatment. However, we developed novel μCAP with 20 mm and 60 mm length can be considered as a local treatment tool and does not exert the systemic therapeutic effects like chemical drugs, meanwhile removing limits of plasma itself. Overall, the above results and discussion indicate that both μCAP with 20 mm and 60 mm length might be useful and should be considered in a clinical medical application.

Conclusions

In this work, we showed that the newly developed micro-sized cold atmospheric plasma (μ CAP) device with 20 mm and 60 mm length stainless steel tubes induce the production of reactive species and radicals in culture medium. There is an increase in the concentration of O_2^- , $\bullet OH$, H_2O_2 , and NO_2^- as a function of μ CAP treatment time, which matches the trend of cell viability of two cancer cells with μ CAP treatment time. A synergistic effect of short- and long-lived species present in the plasma treating DMEM is suspected to play a key role in cell death. Both the 20 and 60 mm length devices have a significant effect on both U87 and MDA-MB-231 cancer cell viability, allowing access to both superficial and deeper tumors. The results of this study suggest a possibility for clinical applications of this micro- μ CAP device on brain and breast tumors. Future work looks to utilize the micro- μ CAP device inside the patient's body.

Reference

- 1 Keidar, M. Plasma for cancer treatment. *Plasma Sources Science and Technology* **24**, 033001 (2015).
- 2 Keidar, M. *et al.* Cold plasma selectivity and the possibility of a paradigm shift in cancer therapy. *British journal of cancer* **105**, 1295-1301 (2011).
- 3 Dezest, M. *et al.* Mechanistic insights into the impact of Cold Atmospheric Pressure Plasma on human epithelial cell lines. *Scientific reports* **7** (2017).
- 4 Cheng, X. *et al.* The effect of tuning cold plasma composition on glioblastoma cell viability. *PloS one* **9**, e98652 (2014).
- 5 Attri, P. *et al.* Influence of ionic liquid and ionic salt on protein against the reactive species generated using dielectric barrier discharge plasma. *Scientific reports* **5**, 17781 (2015).
- 6 Lunov, O. *et al.* Cell death induced by ozone and various non-thermal plasmas: therapeutic perspectives and limitations. *Scientific reports* **4**, 7129 (2014).
- 7 Fridman, G. *et al.* Applied plasma medicine. *Plasma Processes and Polymers* **5**, 503-533 (2008).
- 8 Dikalov, S. I. & Harrison, D. G. Methods for detection of mitochondrial and cellular reactive oxygen species. *Antioxidants & redox signaling* **20**, 372-382 (2014).
- 9 Kalghatgi, S., Friedman, G., Fridman, A. & Clyne, A. M. Endothelial cell proliferation is enhanced by low dose non-thermal plasma through fibroblast growth factor-2 release. *Annals of biomedical engineering* **38**, 748-757 (2010).
- 10 Gjika, E. *et al.* Adaptation Of Operational Parameters Of Cold Atmospheric Plasma And Their Role In Cancer Therapy. *Clinical Plasma Medicine* **9**, 16-17 (2018).
- 11 Vandamme, M. *et al.* Antitumor effect of plasma treatment on U87 glioma xenografts: preliminary results. *Plasma processes and polymers* **7**, 264-273 (2010).
- 12 Chen, Z., Lin, L., Cheng, X., Gjika, E. & Keidar, M. Treatment of gastric cancer cells with nonthermal atmospheric plasma generated in water. *Biointerphases* **11**, 031010 (2016).
- 13 Ishaq, M., Evans, M. M. & Ostrikov, K. K. Effect of atmospheric gas plasmas on cancer cell signaling. *International journal of cancer* **134**, 1517-1528 (2014).
- 14 Hirst, A. *et al.* Low-temperature plasma treatment induces DNA damage leading to necrotic cell death in primary prostate epithelial cells. *British journal of cancer* **112**, 1536-1545 (2015).
- 15 Utsumi, F. *et al.* Effect of indirect nonequilibrium atmospheric pressure plasma on anti-proliferative activity against chronic chemo-resistant ovarian cancer cells in vitro and in vivo. *PloS one* **8**, e81576 (2013).
- 16 Kim, J. Y. *et al.* Apoptosis of lung carcinoma cells induced by a flexible optical fiber-based cold microplasma. *Biosensors and Bioelectronics* **28**, 333-338 (2011).
- 17 Zhang, X., Li, M., Zhou, R., Feng, K. & Yang, S. Ablation of liver cancer cells in vitro by a plasma needle. *Applied Physics Letters* **93**, 021502 (2008).
- 18 Volotskova, O., Hawley, T. S., Stepp, M. A. & Keidar, M. Targeting the cancer cell cycle by cold atmospheric plasma. *Scientific reports* **2**, 636 (2012).
- 19 Chen, Z., Cheng, X., Lin, L. & Keidar, M. Cold atmospheric plasma discharged in water and its potential use in cancer therapy. *Journal of Physics D: Applied Physics* **50**, 015208 (2016).

- 20 Arndt, S. *et al.* Cold atmospheric plasma, a new strategy to induce senescence in melanoma cells. *Experimental dermatology* **22**, 284-289 (2013).
- 21 Georgescu, N. & Lupu, A. R. Tumoral and normal cells treatment with high-voltage pulsed cold atmospheric plasma jets. *IEEE Transactions on Plasma Science* **38**, 1949-1955 (2010).
- 22 Brullé, L. *et al.* Effects of a non thermal plasma treatment alone or in combination with gemcitabine in a MIA PaCa2-luc orthotopic pancreatic carcinoma model. *PloS one* **7**, e52653 (2012).
- 23 Ahn, H. J. *et al.* Atmospheric-pressure plasma jet induces apoptosis involving mitochondria via generation of free radicals. *PloS one* **6**, e28154 (2011).
- 24 Guerrero-Preston, R. *et al.* Cold atmospheric plasma treatment selectively targets head and neck squamous cell carcinoma cells. *International journal of molecular medicine* **34**, 941-946 (2014).
- 25 Chen, Z., Lin, L., Cheng, X., Gjika, E. & Keidar, M. Effects of cold atmospheric plasma generated in deionized water in cell cancer therapy. *Plasma Processes and Polymers* **13**, 1151-1156 (2016).
- 26 Chen, Z. *et al.* Selective treatment of pancreatic cancer cells by plasma-activated saline solutions. *IEEE Transactions on Radiation and Plasma Medical Sciences* **2**, 116-120 (2017).
- 27 Chen, Z., Zhang, S., Levchenko, I., Beilis, I. I. & Keidar, M. In vitro Demonstration of Cancer Inhibiting Properties from Stratified Self-Organized Plasma-Liquid Interface. *Scientific reports* **7**, 12163 (2017).
- 28 Scholtz, V., Julák, J. & Kříha, V. The Microbicidal Effect of Low-Temperature Plasma Generated by Corona Discharge: Comparison of Various Microorganisms on an Agar Surface or in Aqueous Suspension. *Plasma Processes and Polymers* **7**, 237-243 (2010).
- 29 Mirpour, S. *et al.* Utilizing the micron sized non-thermal atmospheric pressure plasma inside the animal body for the tumor treatment application. *Scientific reports* **6**, 29048 (2016).
- 30 Pearse, R. W. B. & Gaydon, A. G. *Identification of molecular spectra*. (Chapman and Hall, 1976).
- 31 Lin, L. & Keidar, M. Cold atmospheric plasma jet in an axial DC electric field. *Physics of Plasmas* **23**, 083529 (2016).
- 32 Sutherland, M. W. & Learmonth, B. A. The tetrazolium dyes MTS and XTT provide new quantitative assays for superoxide and superoxide dismutase. *Free radical research* **27**, 283-289 (1997).
- 33 Bartosz, G. Use of spectroscopic probes for detection of reactive oxygen species. *Clinica Chimica Acta* **368**, 53-76 (2006).
- 34 Satoh, A. Y., Trosko, J. E. & Masten, S. J. Methylene blue dye test for rapid qualitative detection of hydroxyl radicals formed in a Fenton's reaction aqueous solution. *Environmental science & technology* **41**, 2881-2887 (2007).
- 35 Locke, B. R. & Shih, K.-Y. Review of the methods to form hydrogen peroxide in electrical discharge plasma with liquid water. *Plasma Sources Science and Technology* **20**, 034006 (2011).
- 36 Chen, Z. *et al.* A novel micro cold atmospheric plasma device for glioblastoma both in vitro and in vivo. *Cancers* **9**, 61 (2017).

- 37 Graves, D. B. The emerging role of reactive oxygen and nitrogen species in redox biology and some implications for plasma applications to medicine and biology. *Journal of Physics D: Applied Physics* **45**, 263001 (2012).
- 38 Laroussi, M. & Leipold, F. Evaluation of the roles of reactive species, heat, and UV radiation in the inactivation of bacterial cells by air plasmas at atmospheric pressure. *International Journal of Mass Spectrometry* **233**, 81-86 (2004).
- 39 Riedl, S. J. & Shi, Y. Molecular mechanisms of caspase regulation during apoptosis. *Nature reviews Molecular cell biology* **5**, 897-907 (2004).
- 40 Adachi, T. *et al.* Plasma-activated medium induces A549 cell injury via a spiral apoptotic cascade involving the mitochondrial–nuclear network. *Free Radical Biology and Medicine* **79**, 28-44 (2015).
- 41 Boehm, D., Heslin, C., Cullen, P. J. & Bourke, P. Cytotoxic and mutagenic potential of solutions exposed to cold atmospheric plasma. *Scientific reports* **6**, 21464 (2016).
- 42 Arap, W., Pasqualini, R. & Ruoslahti, E. Cancer treatment by targeted drug delivery to tumor vasculature in a mouse model. *Science* **279**, 377-380 (1998).
- 43 Morris, T., Steven Greer, H. & White, P. Psychological and social adjustment to mastectomy. A two-year follow-up study. *Cancer* **40**, 2381-2387 (1977).
- 44 Delaney, G., Jacob, S., Featherstone, C. & Barton, M. The role of radiotherapy in cancer treatment. *Cancer* **104**, 1129-1137 (2005).